Performance Investigation of a Mobile Terminal Phased Array With User Effects at 3.5 GHz for LTE Advanced

Syrytsin, I.; Zhang, S.; Pedersen, Gert F.

Published in:
IEEE Antennas and Wireless Propagation Letters

DOI (link to publication from Publisher):
10.1109/LAWP.2016.2570418

Publication date:
2017

Document Version
Accepted author manuscript, peer reviewed version

Performance Investigation of a Mobile Terminal Phased Array With User Effects at 3.5 GHz for LTE Advanced

Igor Syrytsin, Shuai Zhang, and Gert Frlund Pedersen, *Senior Member, IEEE*

***Abstract*—This letter discusses the performance investigation of a beam-steerable antenna system at 3.5 GHz with user effects. To show how to investigate the performance of such a system, an antenna array system in a metal frame structure is used as one example. The antenna system includes four phased subarrays. Each subarray consists of two slot antenna elements. In the application, it is possible to control the beam by phase in each subarray and switch the main beam direction among the four phased subarrays, depending on the incoming power and interference directions. The main idea in this letter is to evaluate the performance of the phased array system by using the metrics of total scan pattern and coverage efficiency with CTIA standards. The proposed antenna system is simulated and measured in free space and with user effects. Losses in both scan angles and coverage efficiency due to the user effects are also given and discussed in this letter.**

***Index Terms*—LTE advanced, mobile terminal antenna, phased array, user effect.**

I. Introduction

RECENTLY, Long Term Evolution (LTE) band 42 (3.4–3.6 GHz) has been relisted for the application of LTE Advanced [1]. At a frequency of 3.5 GHz, antennas can be made small and directional, thus a phased array could be a feasible solution for the link quality improvement. A system of multiple-phased arrays can improve link quality by applying beamforming in a weak fading environment with a low signal-to-interference-plus-noise ratio (SINR), multibeam multiple-input-multiple-output (MIMO) in a strong fading environment with a high SINR, and diversity in a strong fading environment with a low SINR. This letter will focus on the beamforming capability of the antenna system.

Phased array antenna systems (PAASs) for the mobile terminals have been studied for the frequency higher than 10 GHz in [2]–[5]. In [2], a notch array and a patch array have been proposed. In [3], a linear-phased array antenna has been designed on four layers of the Rogers RT5880 substrates. In [4], an antenna array capable of covering a quarter of the entire space with 11 dBi peak gain is proposed, and, finally, in [5], two integrated mesh-grid patch antenna arrays are illustrated. In [6], a three-dimensional (3-D) beam-steering array has been proposed. However, the mobile terminal-phased array at 3.5 GHz has not been studied before. Different from the frequency higher than 10 GHz, at 3.5 GHz, the radiation patterns of array elements are highly affected by the chassis modes, and thus a radiation pattern depends on the antenna element's location on the ground plane. Furthermore, the body loss has been verified to make big impact on mobile terminal antenna performance [7]. Effects of human body on 3-D radiation patterns have been studied in [8]. In [9], body loss has been studied and reduced by changing the phase between two LTE MIMO antennas at 700 MHz and 1.9 GHz. However, no studies have been done on the performance of a phased array in mobile terminals with the user effects at 3.5 GHz.

In this letter, a performance of the PAAS will be evaluated using the measures of a total scan pattern (TSP) and a coverage efficiency, as described in [2]. The TSP is created by combining all of the radiation patterns for all of the phase shifts. The best achievable gain is extracted at every angular point. The coverage efficiency is extracted from the TSP with respect to the chosen range of the gain values and can be defined as [2]

$$\eta_c = \frac{\text{Coverage Solid Angle}}{\text{Maximum Solid Angle}}. \tag{1}$$

A performance of the PAAS will be studied with the user effect according to the CTIA test plan [10]. A performance is investigated with the two narrow data hand phantoms (dual-hand mode) and a PDA hand phantom (data mode) both in CST Microwave Studio simulations and measurements in the Satimo chamber.

II. Antenna System Geometry

A geometry of the proposed slot PAAS is shown in Fig. 1. The antenna ground plane size is chosen to be $60 \times 120\,\text{mm}^2$. The antenna system consists of a metal frame around the chassis, which is divided into eight slots. The design is symmetrical. The eight slots are distributed into four subarrays as: Array A—slot 1 and slot 2, Array B—slot 3 and slot 4, Array C—slot 5 and slot 6, Array D—slot 7 and slot 8. In the application, the beam is controlled by changing the phase between two slot antennas in each subarray, and the beam can also be switched among four subarrays, depending on the incoming power and interference directions. To compare the proposed PAAS with a conventional antenna system, four reference PAASs are simulated. The reference PAASs geometries are shown in Fig. 2. All reference PAASs are composed of the four phased subarrays, which can be switched ON or OFF, depending on the incoming power direction. Each of the phased arrays consists of one ele-

Manuscript received February 26, 2016; revised April 27, 2016; accepted May 16, 2016. Date of publication May 18, 2016; date of current version March 2, 2017.

The authors are with the Antennas, Propagation and Radio Networking Section, Department of Electronic Systems, Aalborg University, Aalborg 9100, Denmark (e-mail: isyryt11@student.aau.dk; sz@es.aau.dk; gfp@es.aau.dk).

Color versions of one or more of the figures in this letter are available online at http://ieeexplore.ieee.org.

Digital Object Identifier 10.1109/LAWP.2016.2570418

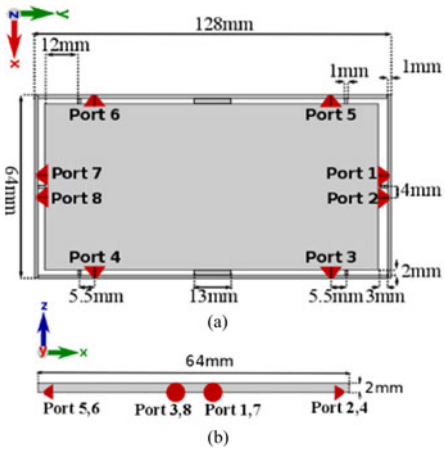

Fig. 1. Geometry of a PAAS in (a) the *xy*-plane and (b) *zy*-plane.

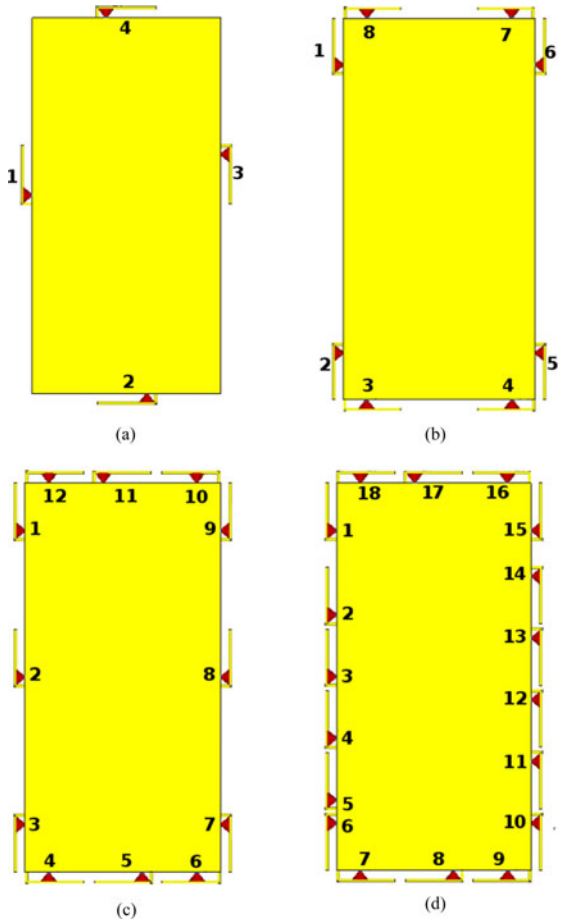

Fig. 2. Setup of a (a) reference PAAS 1, (b) reference PAAS 2, (c) reference PAAS 3, and (d) reference PAAS 4.

ment for the reference PAAS 1, two elements for the reference PAAS 2, and three elements for the reference PAAS 3. In the reference PAAS 4, side arrays consists of six antenna elements. In all of the cases, the antenna element is an inverted-F antenna (IFA), and the triangles correspond to the position of the feeds.

III. Simulations

The -6-dB bandwidth of each antenna in the PAAS is at least 200 MHz at a center frequency of 3.5 GHz. The far-field

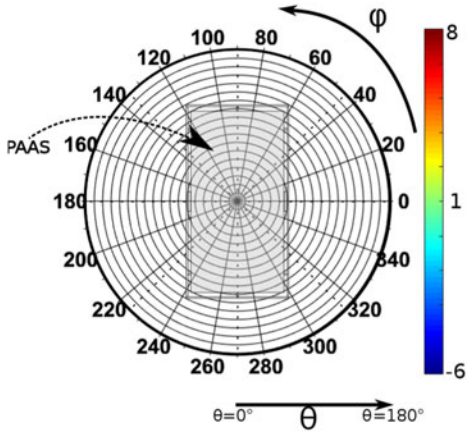

Fig. 3. Mobile phone in the coordinate system, used for plotting far-field results.

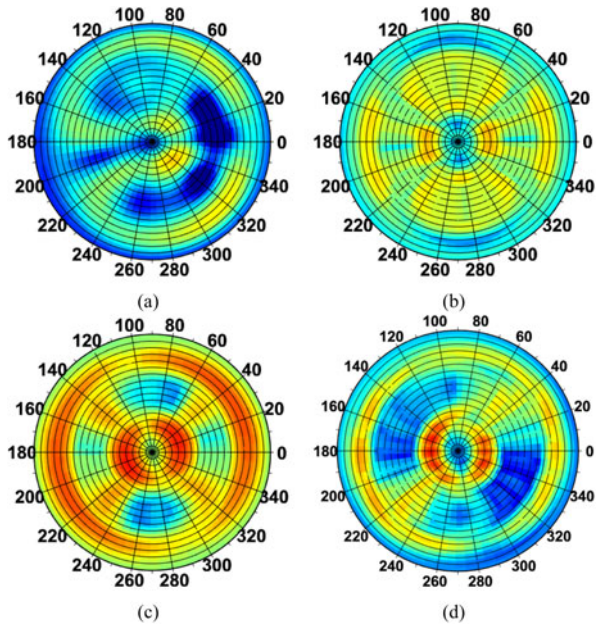

Fig. 4. TSP of the (a) reference PAAS 1, (b) reference PAAS 2, (c) reference PAAS 3, and (d) reference PAAS 4.

results are presented in a 3-D polar plot. The coordinate system of such a plot is shown on Fig. 3. The distance from one circle to another corresponds to the step in θ of 10°. The realized gain of the antenna in dBi is plotted as a color on the top of the 3-D polar plot. The color bar is chosen to range from -6 to 8 dBi, as shown in Fig. 3.

To investigate how an array with resonating frequency of 3.5 GHz will work in the mobile terminal form factor, the four reference arrays are simulated. The TSP of the four reference antenna arrays is shown in Fig. 4. This TSP is composed of four scan patterns—one for each of the subarrays. It can be seen in Fig. 4(b) and (c) at $\phi = 90^\circ$ and $\phi = 270^\circ$ that due to the mutual coupling, the main beam of the dual-element array on the short edge of the ground plane is stronger then the one with the three elements. Therefore, an array of the two elements should be applied on the short edge of the ground plane. Similarly, on the long edge, the maximum number of the elements in an array should be three [see Fig. 4(c) and (d) at $\phi = 90^\circ$, and $\phi = 270^\circ$]. Adding more antenna elements is not proportional to the increase in the gain.

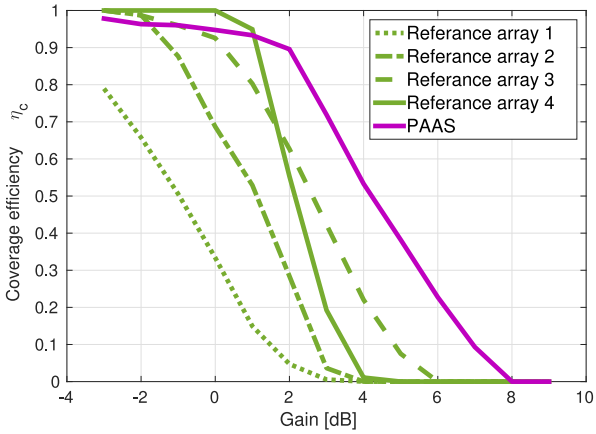

Fig. 5. Simulated coverage efficiency of the reference PAAS and the proposed PAAS.

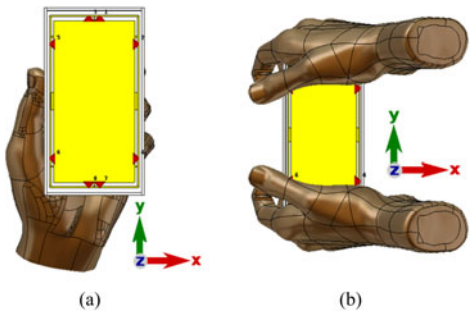

Fig. 6. Simulation setup of (a) data mode and (b) dual-hand mode.

In [11], the slot formed by the ground plane and the metal frame has been used for the lower bands. This slot antenna design has a relatively high radiation efficiency and is insensitive to the user impact [12]; thus, a slot in a metal frame has been used as an array element for the proposed PAAS. In the proposed PAAS design, two slot elements have been used at each edge of the ground plane. To accommodate the lower LTE bands, the proposed PAAS can be reconfigured into the multiband slot antenna [13] by placing a number of RF switches on the frame.

The simulated TSP of the proposed PAAS is shown in Fig. 7(a). A total of eight beams can be seen in Fig. 7(a). Because of the symmetry in the antenna system's geometry, the TSP is totally symmetrical. To see how the proposed PAAS compares in performance to the reference PAASs, the coverage efficiency of each is plotted in Fig. 5. Performance of the PAASs is verified at $\eta_c = 0.7$. As expected, the reference PAAS 1 has the worst performance, as each subarray consists of only one antenna element. The realized gain values for the reference PAAS 2, 3, and 4 are 0, 2, and 2 dBi, correspondingly. It can clearly be seen that an increase in the number of the antenna elements does not always correspond to the increase in the coverage. The gain of a proposed PAAS equals 3 dB at $\eta_c = 0.7$, which is 1 dB better then the best one of the reference PAASs. The slot PAAS also has much simpler implementation, as it only requires one phase shifter with the tuning range from -90° to 90°.

To verify the potential of the proposed PAAS to be used in the mobile terminal, the user effect is included in the simulations, as shown in Fig. 6. A case, made of arlon with $\epsilon_r = 2.5$ and dimensions of $70 \times 135\,\text{mm}^2$, has been constructed to simulate the real case of the mobile terminal and to get at least 3 mm between antenna copper and a user hand.

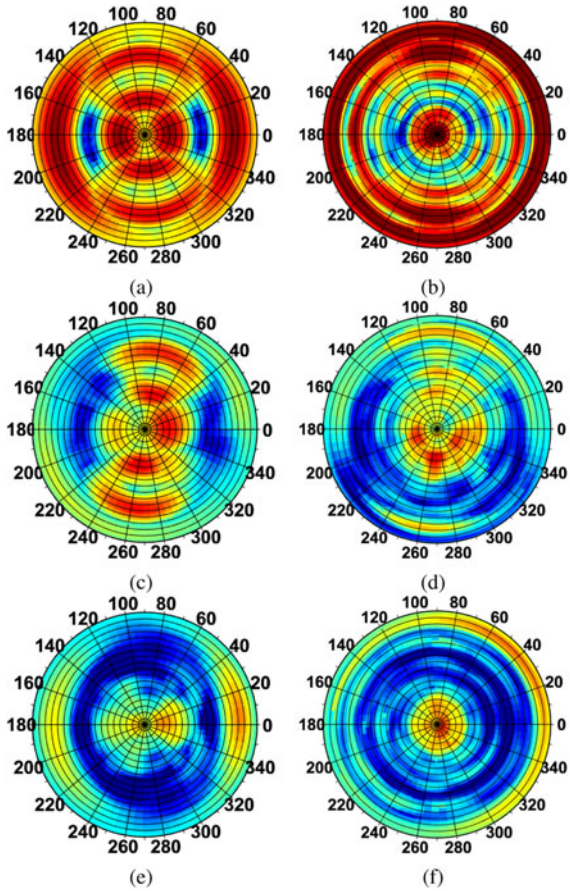

Fig. 7. TSP of the simulated PAAS in (a) free space, (c) data mode, and (d) dual-hand mode. TSP of the measured PAAS in (b) free space, (d) data mode, and (f) dual-hand mode.

Two points are investigated through the simulations with the user impact:

1) change in the TSP of the antenna system due to user effect;
2) change in the coverage efficiency characteristics due to user effect.

The TSP of the proposed PAAS in data mode is shown in Fig. 7(c). In comparison to the simulations without a hand, the TSP is rotated clockwise in ϕ by 10°. The number of strong beams is also reduced to six, and the scan angle of subarray is decreased by at least 10°. The TSP of the PAAS in dual-hand mode is shown in Fig. 7(e), which shows that TSP is reduced to the three strong lobes. Both θ and ϕ scan angles are reduced. Maximum realized gain is also reduced because of the body loss. To investigate the performance of PAAS, coverage efficiency versus realized gain is plotted in Fig. 9. The loss due to the user effect at $\eta_c = 0.7$ is 3 dB for the data mode and 5.5 dB for the dual-hand mode. The highest mutual coupling between the antenna elements is $\leq -13\,\text{dB}$ in free space, $\leq -10\,\text{dB}$ in data mode, and $\leq -15\,\text{dB}$ in dual-hand mode. The coupling results indicate the low correlation, which suggests that PAAS would be able to operate in the multibeam MIMO mode.

IV. Measurements

The prototype of the PAAS is shown in Fig. 8(a), where the discrete ports are replaced by SMA connectors and the PAAS is enclosed in a case. Each antenna is measured separately and then E-field results are combined in MATLAB. The measured

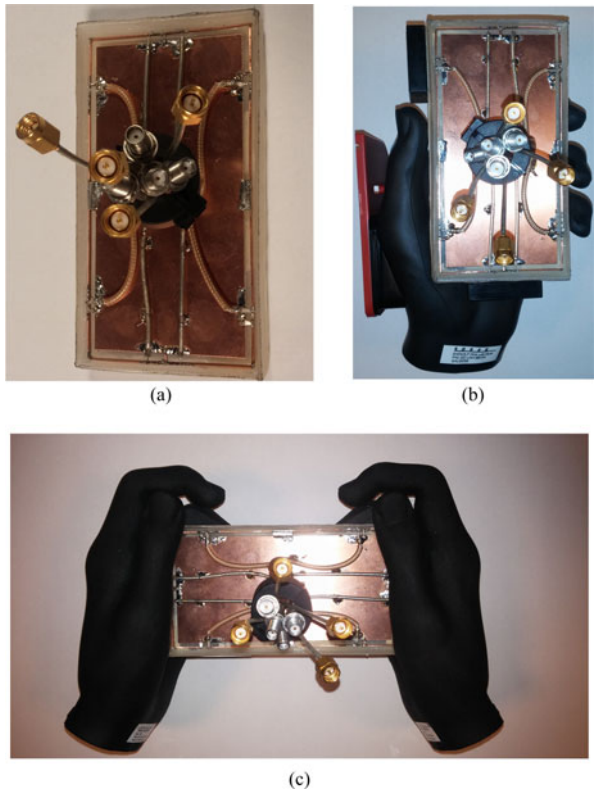

Fig. 8. Measurement setup of the antenna prototype in (a) free space, (b) data mode, and (c) dual-hand mode.

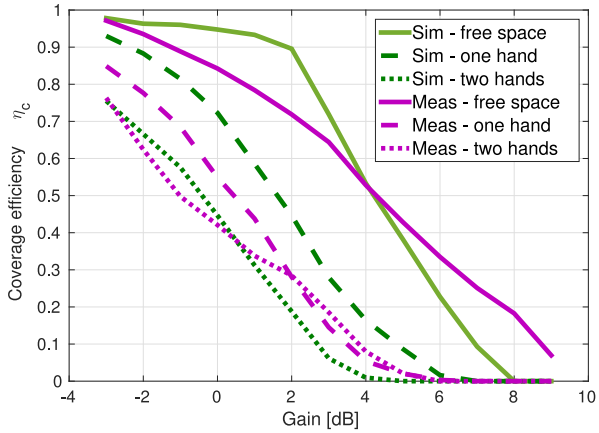

Fig. 9. Coverage efficiency of the measured and simulated PAAS with and without user effect.

TSP of the proposed PAAS is shown in Fig. 7(b). The TSP reassembles one in Fig. 7(a), but the scan angles are smaller and the maximum gain is higher.

A measurement setup in the data mode is shown in Fig. 8(b), and a setup in dual-hand mode is shown in Fig. 8(c). The TSP for the data mode setup is shown in Fig. 7(d). It can clearly be seen that both arrays on the short edge on the ground plane are performing very poorly in comparison to the simulations in Fig. 7(c). The TSP is also rotated clockwise in the same way as in simulations in Fig. 7(c). All of the main beams in the middle of the plot are very weak in comparison to simulations. The TSP for the dual-hand mode setup is shown in Fig. 7(f). The shape of TSP resembles the simulated results in Fig. 7(e) but the maximum gain is higher and the beams in the center of the plot are more narrow. The coverage efficiency is shown in Fig. 9. The measured loss due to the user effect in the data mode is 3 dB at $\eta_c = 0.7$. The measured loss due to the user effect in the dual-hand mode equals 5 dB at $\eta_c = 0.7$. The highest mutual coupling between antenna elements is ≤ -13 dB in all cases for the measured PAAS, which confirms the capability of the PAAS to operate in the multibeam MIMO mode or be used for diversity purposes.

V. Conclusion

It has been shown that a PAAS can be constructed on the chassis of the cellular mobile terminal for the LTE band 42. It has also been shown that the performance of a phased array for 3.5 GHz on the mobile phone ground plane does not always increase with the number of the antenna elements. It can be concluded that the PAAS, designed on the metal frame, used in data mode has at least 3 dB loss at $\eta_c = 0.7$. If the phone is used in the dual-hand mode, a loss of at least 5 dB is to be expected. It can also be concluded that the scan angles of the PAAS will be reused by $10°$–$20°$ in ϕ and up to $40°$ in θ. This letter has shown a method to investigate the performance of the mobile PAAS at 3.5 GHz with a user impact, using the measures of TSP and coverage efficiency.

References

[1] RP-152158, "RAN4 CRS for LTE advanced intra-band contiguous carrier aggregation in band 42 for 4DL," *Nokia Networks, CATT, RAN4#70, Sitges*, Dec. 2015.

[2] J. Helander, K. Zhao, Z. Ying, and D. Sjoberg, "Performance analysis of millimeter wave phased array antennas in cellular handsets," *IEEE Antenna Wireless Propag. Lett.*, vol. 15, pp. 504–507, 2016.

[3] N. Ojaroudiparchin, M. Shen, and G. Pedersen, "Multi-layer 5G mobile phone antenna for multi-user MIMO communications," in *Proc 23rd Telecommun. Forum Telfor*, Nov. 2015, pp. 559–562.

[4] H. Zhou, "Phased array for millimeter-wave mobile handset," in *Proc. Antennas Propag. Soc. Int. Symp.*, Jul. 2014, pp. 933–934.

[5] W. Hong, K. Baek, Y. Lee, and Y. G. Kim, "Design and analysis of a low-profile 28 GHz beam steering antenna solution for future 5G cellular applications," in *Proc. IEEE MTT-S Int. Microw. Symp.*, Jun. 2014, pp. 1–4.

[6] N. Ojaroudiparchin, M. Shen, S. Zhang, and G. Pedersen, "A switchable 3D-coverage phased array antenna package for 5G mobile terminals," *IEEE Antenna Wireless Propag. Lett.*, doi: 10.1109/LAWP.2016.2532607, to be published.

[7] A. Tatomirescu and G. Pedersen, "Body-loss for popular thin smart phones," in *Proc. 7th Eur. Conf. Antennas Propag.*, Apr. 2013, pp. 3754–3757.

[8] J. Krogerus, J. Toivanen, C. Icheln, and P. Vainikainen, "User effect on total radiated power and 3-D radiation pattern of mobile handsets," in *Proc. 1st Eur. Conf. Antennas Propag.*, Nov. 2006, pp. 1–6.

[9] S. Zhang, K. Zhao, Z. Ying, and S. He, "Body loss study of beamforming mode in lte MIMO mobile terminals," in *Proc. 9th Eur. Conf. Antennas Propag.*, Apr. 2015, pp. 1–5.

[10] CTIA Certification, "Test plan for wireless device over the-air performance," no. 3.5.2, 2015.

[11] Y.-L. Ban, Y.-F. Qiang, Z. Chen, K. Kang, and J.-H. Guo, "A dual-loop antenna design for hepta-band WWAN/LTE metal-rimmed smartphone applications," *IEEE Trans. Antennas Propag.*, vol. 63, no. 1, pp. 48–58, Jan. 2015.

[12] K. Zhao, S. Zhang, K. Ishimiya, Z. Ying, and S. He, "Body-insensitive multimode MIMO terminal antenna of double-ring structure," *IEEE Trans. Antennas Propag.*, vol. 63, no. 5, pp. 1925–1936, May 2015.

[13] J. Zhong, K.-K. Chen, and X. Sun, "A novel multi-band antenna for mobile phone with metal frame," in *Proc. 8th Int. Conf. Wireless Commun., Netw. Mobile Comput.*, Sep. 2012, pp. 1–4.